Relation Between the Liquid Spinodal Pressure and the Lateral Pressure Profile at the Liquid-Vapor Interface

Marcello Sega,[1,*] Balázs Fábián[2,3] Attila R. Imre,[4,5] and Pál Jedlovszky,[6,7,*]

[1]*Faculty of Physics, University of Vienna, Boltzmanngasse 5, A-1090 Vienna, Austria*

[2]*Department of Inorganic and Analytical Chemistry, Budapest University of Technology and Economics, Szt. Gellért tér 4, H-1111 Budapest, Hungary*

[3]*Institut UTINAM (CNRS UMR 6213), Université Bourgogne Franche-Comté, 16 route de Gray, F-25030 Besançon, France*

[4]*MTA Centre for Energy Research, P.O. Box 49, H-1525 Budapest, Hungary*

[5]*Department of Energy Engineering, Budapest University of Technology and Economics, Műegyetem rkp. 3, H-1111 Budapest, Hungary*

[6]*Department of Chemistry, Eszterházy Károly University, Leányka utca 6, H-3300 Eger, Hungary*

[7]*MTA-BME Research Group of Technical Analytical Chemistry, Szt. Gellért tér 4, H-1111 Budapest, Hungary*

Running title: Relation Between the Spinodal and the Lateral Pressure Profile

[*]Electronic mail: marcello.sega@univie.ac.at (MS), jedlovszky.pal@uni-eszterhazy.hu (PJ)

Abstract

Computer simulations of the liquid-vapor interface of the Lennard-Jones fluid and SPC/E water are performed on the (N,V,T) ensemble at various temperatures, in order to compare the minimum of the lateral pressure profile with the spinodal pressure. Our results show that these two pressures agree within error bars for water in a rather broad range of temperatures, but only a proportionality of these values are found in the case of the Lennard-Jones system. Our results might offer a novel tool to estimate the spinodal line in situations of practical relevance.

1. Introduction

The spinodal line represents the limit of mechanical stability of a phase on the temperature (T) - pressure (p) phase diagram.[1] The liquid-vapor coexistence curve marks the limit of thermodynamic stability of the liquid phase, beyond which the liquid state no longer corresponds to the global minimum of the free energy. However, the liquid state can still exist beyond the liquid-vapor coexistence curve in the form of superheated liquid, a state that is metastable (i.e., it corresponds to a local minimum of the free energy) with respect to the vapor phase. This metastable region extends from the liquid-vapor coexistence curve to the liquid spinodal line, which starts from the critical point and goes below the coexistence line in the T-p phase diagram. Beyond the spinodal line, the liquid phase cannot exist even as a metastable state, because it no longer corresponds to a minimum of the free energy.[1]

Approximating the location of the liquid spinodal line as accurately as possible is of great relevance both from the point of view of pure science and from that of the applications. Thus, for instance, the shape of this spinodal line (i.e., being re-entrant[2,3] or not[4-9]) can be related to the origin of a number of anomalous features of supercooled water. On the other hand, knowing the exact location of the spinodal is also of great importance in any process that involves metastable states. For example, when the pressure drop or temperature increase is very fast, near-spinodal states can be reached before nucleation takes place. This can happen during the breaking of high pressure-high temperature pipelines (such as the cooling circle of a power plant, or the storage tank of a compressed gas), resulting in a sudden and violent phase transition, the so-called explosive or flash boiling.[10-12] Similar near-spinodal states can be reached when the liquid comes into contact with hot material (e.g., magma or molten metal). Although, from the physical point of view, the sudden boiling following the

contact does not differ from the previously mentioned process, in this case it is often referred to as "steam explosion".[13] Finally, even near-spinodal states with negative pressure can be reached when high-amplitude pressure waves (for example, medical ultrasound) are applied in a liquid-containing environment, causing very rapid and violent cavitation or "embolism", a potential risk for neighboring materials, such as human tissues.[14] However, the spinodal line is experimentally almost inaccessible in common fluids, because upon approaching the spinodal, the liquid state becomes increasingly metastable with respect to the vapor phase, and hence the unavoidable presence of even an otherwise negligible amount of impurities leads to sudden evaporation, bringing the system to the thermodynamically stable vapor phase before the spinodal can be reached.

The liquid spinodal of a model system can, on the other hand, be accessed by computer simulation methods. Thus, as it was suggested by Poole et al. more than two decades ago, at a given temperature the pressure goes through a minimum as a function of the density (ρ); the spinodal pressure is simply the value of this minimum.[4,5] This method has been applied to determine the liquid spinodal of various water models[4,5,7-9] as well as that of the Lennard-Jones system[15] and liquid SiO2.[16] However, similarly to the vast majority of the equations of state, potential models are also typically parametrized by fitting data corresponding to the thermodynamically stable liquid state, and hence their performance at deeply superheated and/or negative pressure states is not fully justified. Therefore, it is desirable to relate the spinodal pressure to experimentally accessible quantities, making thus the spinodal line of real liquids also accessible.

Recently, Imre et al. conjectured that the pressure of the liquid spinodal at a given temperature is closely related to the minimum value of the lateral pressure profile, $p(X)$, across the liquid-vapor interface of the same system at the same temperature.[17] This estimation of the spinodal line, called the 'interfacial spinodal', of liquid helium, the only

simple liquid for which the spinodal can be experimentally accessed with reasonable accuracy, did not provide incompatible results with experimental data.[18] They also determined the interfacial spinodal of the Lennard-Jones fluid[17] and of CO2,[19] and found them closely related to the spinodal line obtained from certain equations of state. Further, they also determined the interfacial spinodal of water, and used this result to distinguish between the performances of various equations of state.[12]

The idea that the knowledge of the equation of state in the unstable region, between the liquid and vapor densities, can give access to the density profile, $\rho(X)$, of a liquid-vapor interface, is not new and dates back to Rayleigh.[20] In particular, if the two profiles $p(X)$ and $\rho(X)$ are known, and the latter is invertible, one can, through the function $X(\rho)$, obtain the equation-of-state $p(\rho)$. According to the conjecture of Imre et al., the pressure along the spinodal line is then related to the most negative value the pressure profile can take.[17] In the light of these considerations it is interesting to test the hypothesis of Imre et al.,[17] and to check if the spinodal pressure and the minimum value of the lateral pressure profile can indeed be related to each other. For this purpose, we compare these quantities for the Lennard-Jones fluid and for the SPC/E model[21] of water. For the Lennard-Jones fluid, we calculate the spinodal pressure in the conventional way, while for water we take it from the literature,[7] and compare them with those of the interfacial spinodal determined here.

2. Computational Details

2.1. Molecular Dynamics Simulations. To determine the liquid spinodal of the Lennard-Jones fluid we have performed a set of molecular dynamics (MD) simulations on the canonical (N,V,T) ensemble with 2048 Lennard-Jones particles placed in a cubic basic box at 6 different temperatures, performing simulations at 8-10 different densities at each

temperature. The temperatures (in terms of reduced units) considered are ranging from 0.7 to 0.95 with a spacing of 0.05. The temperature range has been chosen to be between the triple point temperature and critical temperature of the Lennard-Jones fluid, which are 0.694[22] and 1.326,[23] respectively. However, at temperatures above 0.95 we observed bubble formation in the liquid phase of the interfacial system; hence these temperatures have been discarded. At each temperature, we started with a simulation at $\rho^* = 0.78$, and progressively decreased the density below the value at which we found a minimum of the pressure. Simulations performed below the lowest density reported in Figure 1 have led to the immediate disappearance of the metastable homogeneous liquid phase, with a consequent bubble formation. (For convenience, we use here reduced units of the temperature, number density, and pressure, i.e., $T^* = k_B T/\varepsilon$, $\rho^* = \rho\sigma^3$, and $p^* = p\sigma^{-3}/\varepsilon$, respectively, where k_B is the Boltzmann constant, and σ and ε are the Lennard-Jones distance and energy parameters, respectively.) The values of the Lennard-Jones interaction parameters have been set to $\sigma = 3.4$ Å and $(\varepsilon/k_B) = 120$ K, respectively, while the mass of the particles has been 40 a.m.u, corresponding to the argon model of Rahman.[24]

To compute the interfacial spinodal, we have performed MD simulations of the liquid-vapor interface of the Lennard-Jones system and of water on the canonical (N,V,T) ensemble at the temperature values at which the spinodal was determined. It should be noted that for water this temperature range is particularly relevant in relation to the explanation of the anomalous features of supercooled water.[2-9] In describing water molecules, the SPC/E model[21] has been used, since the spinodal of this model has already been determined in the literature.[7] SPC/E is a three-site model, bearing fractional charges of -0.8476 e and 0.4238 e at the O and H atoms, respectively, the O atom being the also center of a Lennard-Jones interaction with distance and energy parameters $\sigma = 3.166$ Å and $\varepsilon = 0.65$ kJ/mol, respectively. The distance of the H and O atoms is 1.0 Å, while the H-O-H angle is 109.47°.[21]

The triple point and critical point of this water model correspond to the temperature values of about 215 K[25] and 652 K,[26] respectively. The rectangular basic box in the interfacial simulations has contained 2237 Lennard-Jones particles or 4000 water molecules, having the *X*, *Y*, and *Z* edge lengths of 180, 40, and 40 Å long, respectively, for the Lennard-Jones system, and of 300, 50, and 50 Å, respectively, for water, *X* being the interface normal. All simulations have been done with an in-house modified version of the GROMACS 5.1 program package[27] that calculates also the pressure contribution of each particle.[28] All interactions have been truncated to zero beyond the cut-off distance of 11 Å; their long range part has been accounted for using the smooth Particle Mesh Ewald method[29] for the Coulomb interaction in water as well as for the van der Waals dispersion in the Lennard-Jones system, with the accuracy of the reciprocal space contribution of 10^{-5} and 5×10^{-4}, respectively. In should be noted that taking the long-range part of the van der Waals interaction into account using an Ewald-based method is particularly important in the presence of an interface, as in this case the anisotropy of the system prevents the use of the analytical tail correction.[30] The temperature of the systems has been controlled by means of the Nosé-Hoover thermostat.[31,32] The geometry of the water molecules has been kept fixed using the SHAKE algorithm.[33] Equations of motion have been integrated in time steps of 1 fs. Bulk Lennard-Jones and interfacial systems have been equilibrated for at least 100 ps and 1 ns, respectively. The value of the pressure (in the bulk Lennard-Jones simulations) and the lateral pressure profile (in the interfacial simulations) have then been evaluated over 200 ps and 5 ns long equilibrium trajectories, respectively.

2.2. Calculation of the Lateral Pressure Profile. The calculation of the profile of the lateral pressure is not a trivial task, as it requires the localization of an inherently non-local quantity. Thus, the pressure contribution of the interaction of an atom pair is given as a contour integral along an open path C_{ij} connecting the two interacting atoms *i* and *j*:[34]

$$p_{\mu\nu}(\mathbf{r}) = \frac{1}{V}\left(\sum_{ij} f_{ij}^{\mu} \int_{C_{ij}} ds^{\nu}\, \delta(\mathbf{r}-\mathbf{s}) + \sum_{i} m_i v_i^{\mu} v_i^{\nu} \right),$$

where $p_{\mu\nu}$ are the components of the pressure tensor, f_{ij} is the force between the two atoms, V is the volume, **s** is the position of the path element, and m_i and v_i are the mass and velocity, respectively, of particle i. Among the possible choices of the path C_{ij} that provide compatible results,[35] we have chosen the Harasima contour,[36] in which the path is composed of two segments, one being parallel with the surface, and the other one perpendicular to it (see Fig. 6 of Ref. 37). The choice of this path was dictated by two reasons. First, this way the lateral pressure can simply be distributed among the atomic positions in the system, which makes the pressure profile calculation computationally very efficient.[37] Second, this path can be used in calculating the lateral pressure profile even if the potential energy of the system is not pairwise additive.[35] The importance of this point becomes evident considering that even if the intermolecular potential function is pairwise additive, the reciprocal space part of the long range correction of the potential energy, occurring in Ewald summation[38,39] and its particle mesh variants[29,40] cannot be written as a sum over particle pairs. To account for this reciprocal space term of the sPME contribution we have used the method that was recently developed by us.[41]

3. Results and Discussion

Figure 1 shows the pressure vs. density data obtained for the Lennard-Jones system at different temperatures. The spinodal pressure was simply regarded as the smallest of the obtained pressures along the given isotherm; its values obtained at different temperatures along with the corresponding densities are collected in Table 1. In determining the pressure in

these highly metastable systems we had to check carefully whether the system remained homogeneous in the entire course of the simulation. We monitored this both by following the time evolution of the pressure in the system and also by visual inspection of the configurations. In the case of bubble formation, happening typically upon approaching the spinodal, the pressure, previously fluctuating around a constant value, starts drifting to less negative values, as shown in Figure 2, indicating the transition from a homogeneous metastable to a thermodynamically stable two-phase system. In such cases the pressure of the metastable homogeneous liquid was extracted by averaging only over the time range preceding the bubble formation, given that the metastable state persisted long enough to perform a meaningful averaging of the pressure. At even lower densities bubble formation occurred instantaneously, preventing us thus from calculating the metastable pressure. Fortunately, this always happened below the density where the pressure showed a minimum.

The lateral pressure profiles, obtained across the liquid-vapor interface of the Lennard-Jones fluid and water, are shown in Figure 3. a and b, respectively. The profiles are constant in the bulk vapor phase, and fluctuate around the same value in the bulk liquid phase, indicating that the two phases are indeed in equilibrium with each other. All the profiles exhibit a clear, deep minimum at the liquid side of the interface. The profiles shown are not symmetrized over the two interfaces present in the basic box; the difference between the two minimum values at the two interfaces can thus serve us as an estimate of the uncertainty of the obtained interfacial spinodal values. The obtained minimum of the lateral pressure profiles are compared with the spinodal pressure values in Figure 4. a and b for the Lennard-Jones fluid and water, respectively. As is seen, for water the spinodal pressure almost always agrees with the minimum value of the lateral pressure profile within error bars. The slight, few MPa difference observed at 280 K can easily be explained by the slightly different simulation setup used in the two calculations. The picture is, however, completely different for the Lennard-

Jones fluid. Here the minimum value of the lateral pressure profile is consistently higher, but follows the same trend as the spinodal pressure in the entire temperature range studied. Moreover, the ratio of these two pressure values turns out to be around 1.65 in every case.

The observed different behavior of water and the Lennard-Jones fluid cannot simply be explained by the difference of the temperature ranges studied from the melting or critical point, because we found the ratio of the spinodal pressure and minimum of the lateral pressure profile temperature independent in both cases. Further, the range of temperatures studied starts right at the triple point temperature for both systems. Instead, it should be considered that the hypothesized equivalence of the minimum value of the lateral pressure in the interfacial system and of the spinodal pressure can be derived assuming the equivalence of the local free energy density in the interfacial system with that of a homogeneous system at the same density. However, for thermodynamic consistency, this equation needs to be supplemented with a term depending on the gradient of the density itself.[42] This fact could, in principle, be at the origin of the observed behavior, suggesting that this term is negligible for water but cannot be neglected in the case of the Lennard-Jones system.

4. Conclusions

Summarizing, our results do not confirm, in general, the conjecture that the liquid spinodal can well be approximated with the minimum of the lateral pressure profile at the liquid-vapor interface. The two pressures are, nevertheless, found to be proportional with each other, their ratio being system dependent. This proportionality implies that the spinodal line could be reconstructed, if its value is known from an independent source at one single temperature (knowing also the critical point, i.e., the endpoint of the spinodal line). Such an independent source can be, e.g., the approximation of the spinodal with the experimentally

measurable limit of overheat.[43] Finally, it should also be noted that although the approximation of the spinodal pressure by the minimum of the interfacial lateral pressure profile was not found to work in general, it works well in the case of water, the particular liquid for which knowing at least the approximate location of the liquid spinodal is of far the greatest practical importance. Thus, the present results provide also a simple way of estimating the spinodal pressure of water both for practical applications and for fine tuning parameters in appropriate equations-of-state.

Acknowledgements. This work has been supported by the Hungarian NKFIH Foundation under Project No. 119732, and by the Action Austria-Hungary Foundation under project No. 93öu3. The calculations have been performed using the Vienna Scientific Cluster (VSC).

References

(1) Stanley, H. E. *Introduction to Phase Transitions and Critical Phenomena*; Oxford University Press: Oxford, 1971.

(2) Speedy, R. J.; Angell, C. A. Isothermal Compressibility of Supercooled Water and Evidence for a Thermodynamic Singularity at -45^{o}C. *J. Chem. Phys.* **1976**, *65*, 851-858.

(3) Speedy, R. J. Stability-Limit Conjecture. An Interpretation of the Properties of Water. *J. Phys. Chem*. **1982,** *86*, 982-991.

(4) Poole, P. H.; Sciortino, F.; Essmann, U.; Stanley, H. E. Phase Behaviour of Metastable Water. *Nature* **1992,** *360*, 324-328.

(5) Poole, P. H.; Sciortino, F.; Essmann, U.; Stanley, H. E. Spinodal of Liquid Water, *Phys. Rev. E* **1993,** *48*, 3799-3817.

(6) Sastry, S.; Debenedetti, P. G.; Sciortino, F.; Stanley, H. E. Singularity-Free Interpretation of the Thermodynamics of Supercooled Water. *Phys. Rev. E* **1996,** *53*, 6144-6154.

(7) Netz, P. A.; Starr, F. W.; Stanley, H. E.; Barbosa, M. C. Static and Dynamic Properties of Stretched Water. *J. Chem. Phys.* **2001,** *115*, 344-348.

(8) Yamada, M.; Mossa, S.; Stanley, H. E.; Sciortino, F. Interplay Between Time-Temperature Transformation and the Liquid-Liquid Phase Transition in Water. *Phys. Rev. Letters* **2002,** *88*, 195701-1-4.

(9) Gallo, P.; Minozzi, M.; Rovere, M. Spinodal of Supercooled Polarizable Water, *Phys. Rev. E* **2007,** *75*, 011201-1-7.

(10) Abbasi, T.; Abbasi, S. A. Accidental Risk of Superheated Liquids and a Framework for Predicting the Superheat Limit. *J. Loss Prevention in Proc. Ind.* **2007,** *20*, 165-181.

(11) Poullikkas, A. Effects of Two-Phase Liquid-Gas Flow on the Performance of Nuclear Reactor Cooling Pumps. *Progr. Nucl. Energy* **2003,** *42*, 3-10.

(12) Imre, A. R.; Baranyai, A.; Deiters, U. K.; Kiss, P. T.; Kraska, T.; Quiñones Cisneros, S. E. Estimation of the Thermodynamic Limit of Overheating for Bulk Water from Interfacial Properties. *Int. J. Thermophys.* **2013,** *34*, 2053-2064.

(13) Lamome, J.; Meignen, R. On the Explosivity of a Molten Drop Submitted to a Small Pressure Perturbation, *Nucl. Engin. Design* **2008,** *238*, 3445-3456.

(14) Nakabaru, T.; Hashimoto, T.; Matsuo, S.; Setoguchi, T.; Rajesh, G. Generating and Focusing of Underwater Expansion Wave Using a Silicon Resin Reflector. *J. Thermal Sci*. **2013,** *22,* 209-215.

(15) Baidakov, V. G.; Protsenko, S. P. Metastable States in Liquid-Gas Phase Transition. Simulation by the Method of Molecular Dynamics. *High Temperature* **2003,** *41*, 195-200.

(16) Stanley, H. E.; Angell, C. A.; Essmann, U.; Hemmati, M.; Poole, P. H.; Sciortino, F. Is There a Second Critical Point in Liquid Water? *Physica A* **1994,** *205*, 122-139.

(17) Imre, A. R.; Mayer, G.; Házi, G.; Rozas, R.; Kraska, T. Estimation of the Liquid-Vapor Spinodal from Interfacial Properties Obtained from Molecular Dynamics and Lattice Boltzmann Simulations. *J. Chem. Phys.* **2008,** *128*, 114708-1-11.

(18) Imre, A. R.; Kraska, T. Liquid-Vapour Spinodal of Pure Helium 4, *Physica B* **2008,** *403*, 3663-3666.

(19) Kraska, T.; Römer, F.; Imre, A. R. The Relation of Interface Properties and Bulk Phase Stability: Molecular Dynamics Simulation of Carbon Dioxide. *J. Phys. Chem. B* **2009,** *113*, 4688-4697.

(20) Rayleigh, L. On the Theory of Surface Forces. - II. Compressible Fluids. *Phil. Mag. Ser. 5* **1892,** *33*, 209-220.

(21) Berendsen, H. J. C.; Grigera, J. R.; Straatsma, T. The Missing Term in Effective Pair Potentials. *J. Phys. Chem.* **1987,** *91*, 6269-6271.

(22) Mastny, E. A.; de Pablo, J. J. Melting Line of the Lennard-Jones System, Infinite Size, and Full Potential. *J. Chem. Phys*. **2007,** *127*, 104504-1-8.

(23) Caillol, J. M. Critical-Point of the Lennard-Jones Fluid: A Finite Size Scaling Study. *J. Chem. Phys*. **1998,** *109*, 4885-4893.

(24) Rahman, A. Correlations in the Motion of Atoms in Liquid Argon. *Phys. Rev.* **1964,** *136*, A405-A411.

(25) Bryk, T.; Haymet, A. D. J. The Ice/Water Interface: Density-Temperature Phase Diagram for the SPC/E Model of Liquid Water. *Mol. Simul.* **2004,** *30*, 131-135.

(26) Guillot, B.; Guissani, Y. How To Build A Better Pair Potential for Water. *J. Chem. Phys*. **2001,** *114*, 6720-6733.

(27) Pronk, S.; Páll, S.; Schulz, R.; Larsson, P.; Bjelkmar, P.; Apostolov, R.; Shirts, M. R.; Smith, J. C.; Kasson, P. M.; van der Spoel; D., et al. GROMACS 4.5: A High-Throughput and Highly Parallel Open Source Molecular Simulation Toolkit. *Bioinformatics* **2013,** *29*, 845–854.

(28) The code is freely available at https://github.com/Marcello-Sega/gromacs/tree/virial/.

(29) Essman, U.; Perera, L.; Berkowitz, M. L.; Darden, T.; Lee, H.; Pedersen, L. G. A Smooth Particle Mesh Ewald Method. *J. Chem. Phys.* **1995,** *103*, 8577-8594.

(30) in't Veld, P. J.; Ismail, A. E.; Grest, G. S. Application of Ewald Summations to Long–Range Dispersion Forces. *J. Chem. Phys*. **2007,** *127*, 144711-1-8.

(31) Nosé, S. A Molecular Dynamics Method for Simulations in the Canonical Ensemble. *Mol. Phys.* **1984,** *52*, 255-268.

(32) Hoover, W. G. Canonical Dynamics: Equilibrium Phase-Space Distributions. *Phys. Rev. A* **1985,** *31*, 1695-1697.

(33) Ryckaert, J. P.; Ciccotti, G.; Berendsen, H. J. C. Numerical Integration of the Cartesian Equations of Motion of a System With Constraints; Molecular Dynamics of n-Alkanes. *J. Comp. Phys.* **1977,** *23*, 327–341.

(34) Schofield, P.; Henderson, J. R. Statistical Mechanics of Inhomogeneous Fluids. *Proc. R. Soc. Lond. A* **1982,** *379*, 231-246.

(35) Sonne, J.; Hansen, F. Y.; Peters, G. H. Methodological Problems in Pressure Profile Calculations for Lipid Bilayers. *J. Chem. Phys.* **2005,** *122*, 124903-1-9.

(36) Harasima, A. Molecular Theory of Surface Tension. *Adv. Chem. Phys.* **1958,** *1*, 203-237.

(37) Sega, M.; Fábián, B.; Jedlovszky, P. Layer-by-Layer and Intrinsic Analysis of Molecular and Thermodynamic Properties Across Soft Interfaces. *J. Chem. Phys.* **2015,** *143*, 114709-1-8.

(38) Ewald, P. Die Berechnung Optischer und Elektrostatischer Gitterpotentiale. *Ann. Phys.* **1921,** *369*, 253–287.

(39) de Leeuw, S. W.; Perram, J. W.; Smith, E. R. Simulation of Electrostatic Systems in Periodic Boundary Conditions. I. Lattice Sums and Dielectric Constants. *Proc. R. Soc. Lond. A* **1980,** *373*, 27-56.

(40) Darden, T.; York, D.; Pedersen, L. Particle Mesh Ewald: An N·log(N) Method for Ewald Sums in Large Systems. *J. Chem. Phys.* **1993,** *98*, 10089-10092.

(41) Sega, M.; Fábián, B.; Jedlovszky, P. Pressure Profile Calculation with Particle Mesh Ewald Methods. *J. Chem. Theory Comput*. **2016,** *12*, 4509-4515.

(42) Rowlinson, J. S.; Widom, B. *Molecular Theory of Capillarity*; Dover Publications: Mineola, 2002, p. 52.

(43) Puchinskis, S. E.; Skripov, P. V. The Attainable Superheat: From Simple to Polymeric Liquids. *Int. J. Thermophys.* **2001,** *22*, 1755-1768.

Tables

TABLE 1. Spinodal Data of the Lennard-Jones Fluid

T^*	0.70	0.75	0.80	0.85	0.90	0.95
p^*	-0.99	-0.81	-0.71	-0.55	-0.46	-0.35
ρ^*	0.69±0.005	0.68±0.015	0.66±0.01	0.66±0.01	0.64±0.01	0.63±0.01

Figure legend

Figure 1. Dependence of the pressure of the Lennard-Jones fluid on the density at the six temperatures considered. The profiles corresponding to the reduced temperature values of 0.75, 0.8, 0.85, 0.9, and 0.95 are shifted by 0.15, 0.3, 0.45, 0.6, and 0.75 units for clarity. Error bars are only shown when larger than the symbols.

Figure 2. Time evolution of the pressure in the simulation of the bulk Lennard-Jones fluid, performed at the reduced temperature and density values of 0.7 and 0.71, respectively. The arrow marks the point where bubble formation occurs.

Figure 3. Lateral pressure profile of (a) the Lennard-Jones fluid, and (b) SPC/E water along the liquid-vapor interface normal axis, as obtained at different temperatures. For the Lennard-Jones fluid, the profiles corresponding to the reduced temperature values of 0.75, 0.8, 0.85, 0.9, and 0.95 are shifted by 0.15, 0.3, 0.45, 0.6, and 0.75 units, whereas for water, the profiles corresponding to 230 K, 240 K, 250 K, 260 K, and 280 K are shifted by 150 MPa, 300 MPa, 450 MPa, 600 MPa, and 750 MPa, for clarity.

Figure 4. Comparison of the spinodal pressure of (a) the Lennard-Jones fluid and (b) SPC/E water (Ref. 7), shown by black dots, with the obtained minimum of the interfacial lateral pressure profile (red dots) at various temperatures. Error bars are only shown when larger than the symbols.

Figure 1

Sega et al.

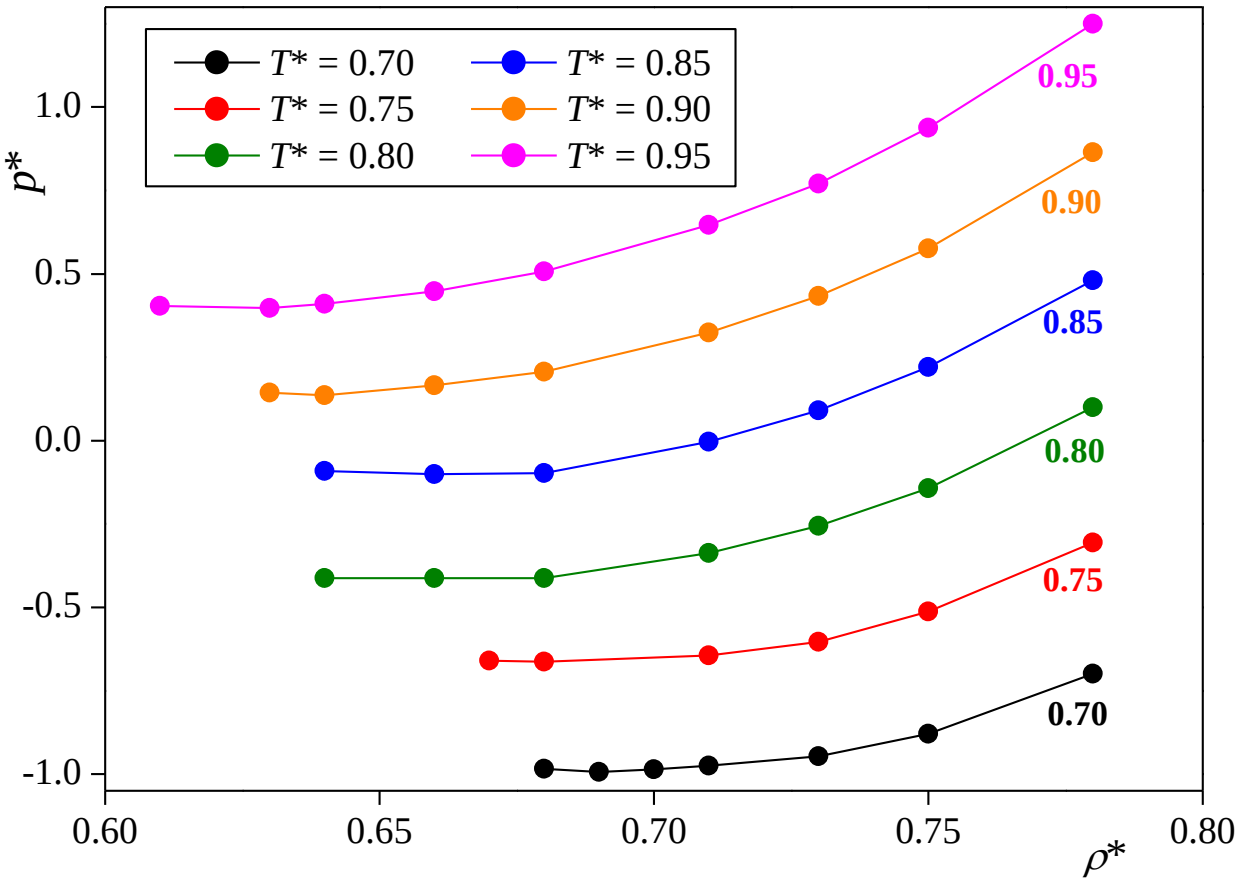

Figure 2

Sega et al.

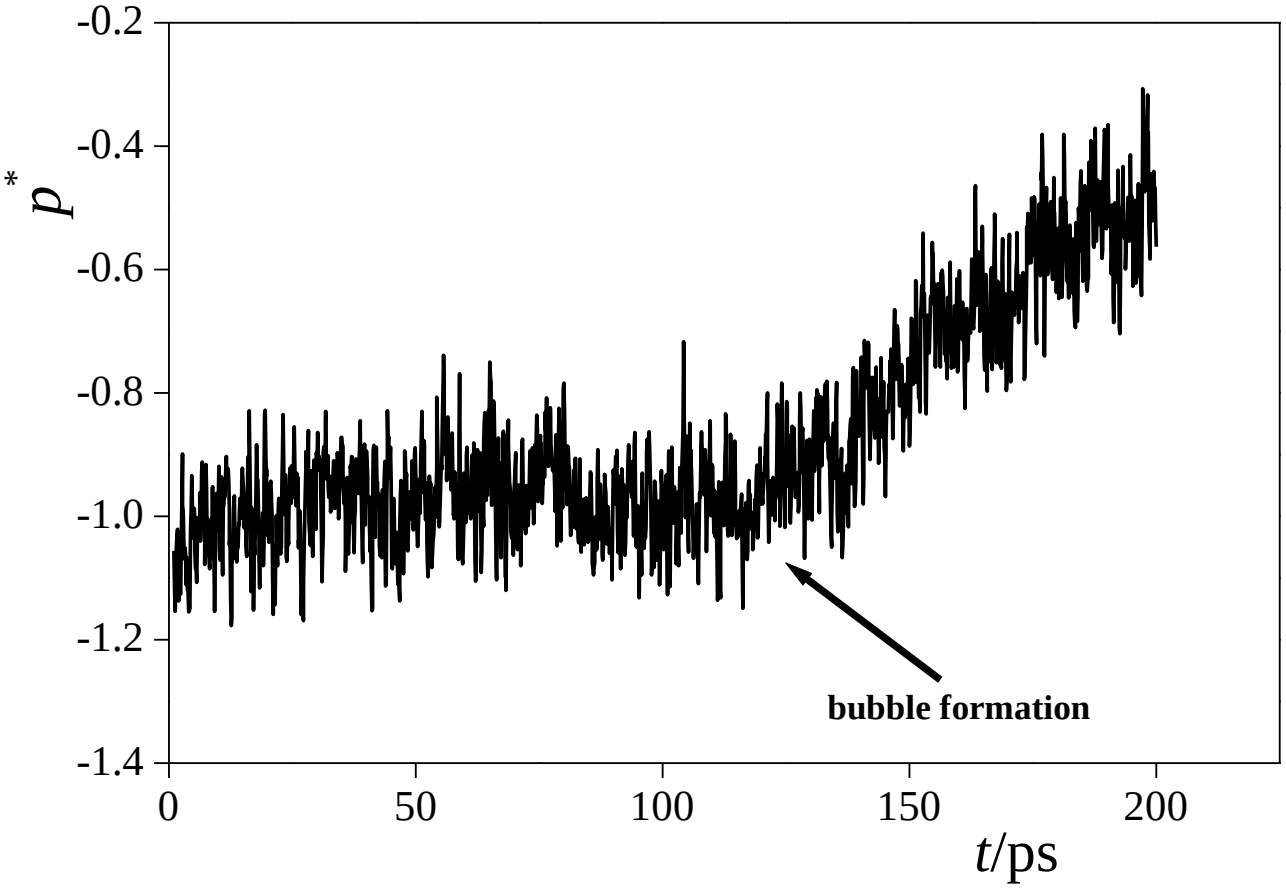

Figure 3.a

Sega et al.

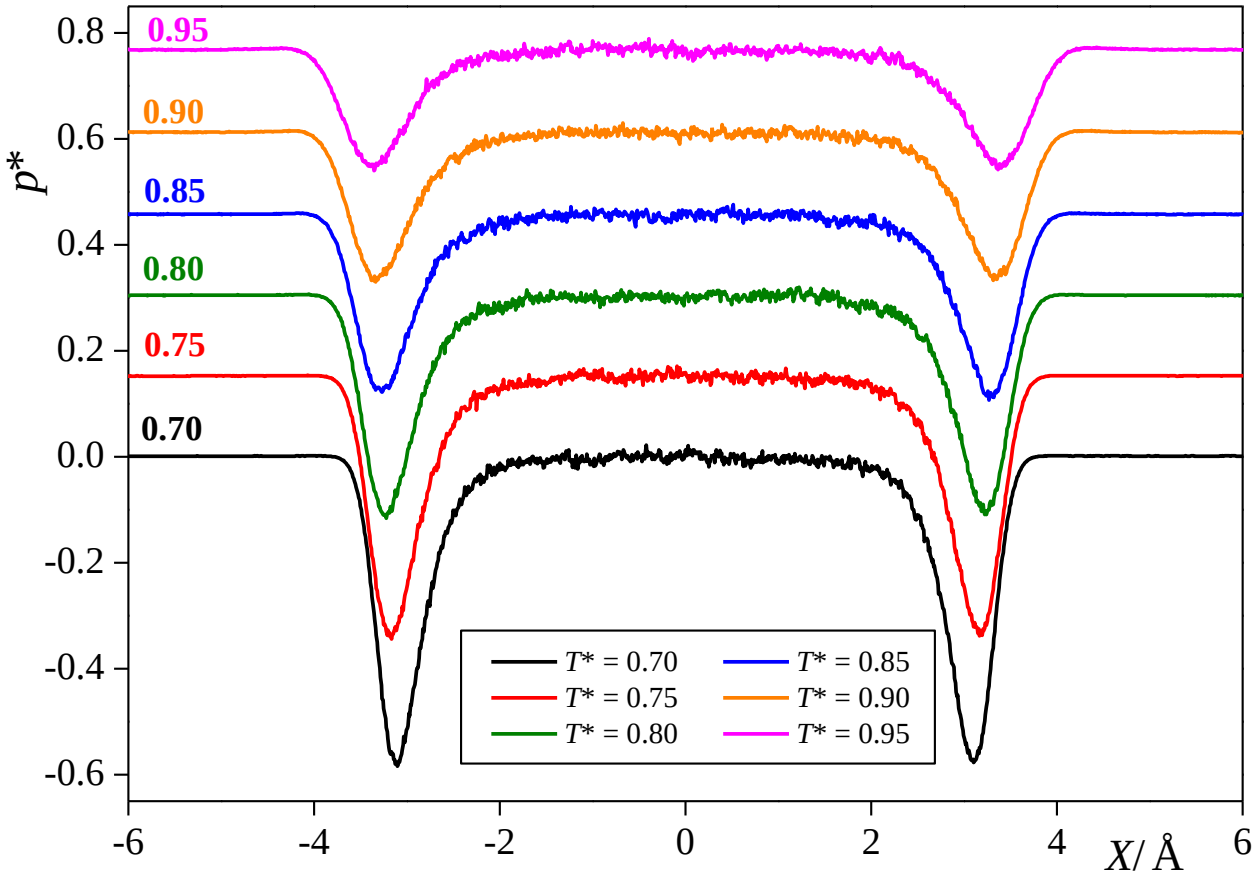

Figure 3.b

Sega et al.

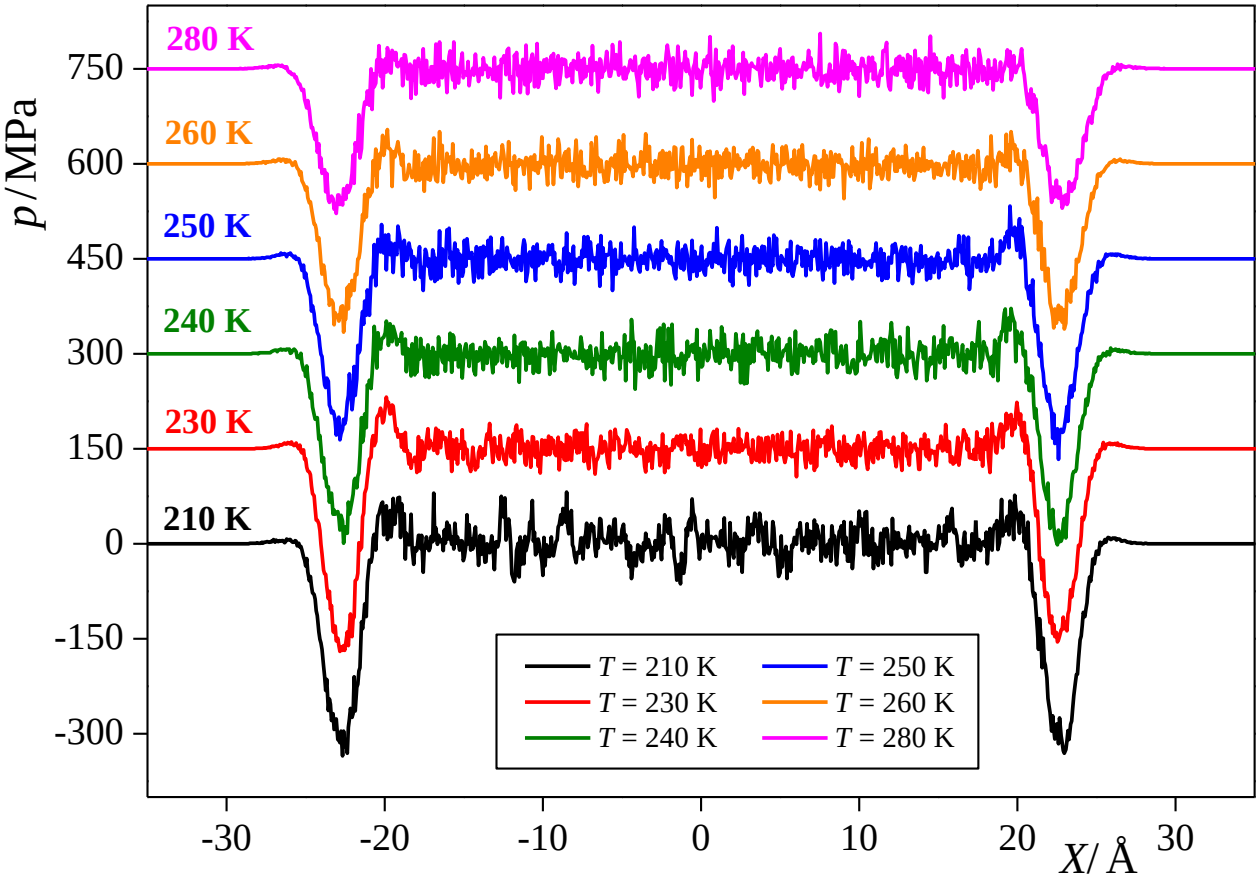

Figure 4.

Sega et al.

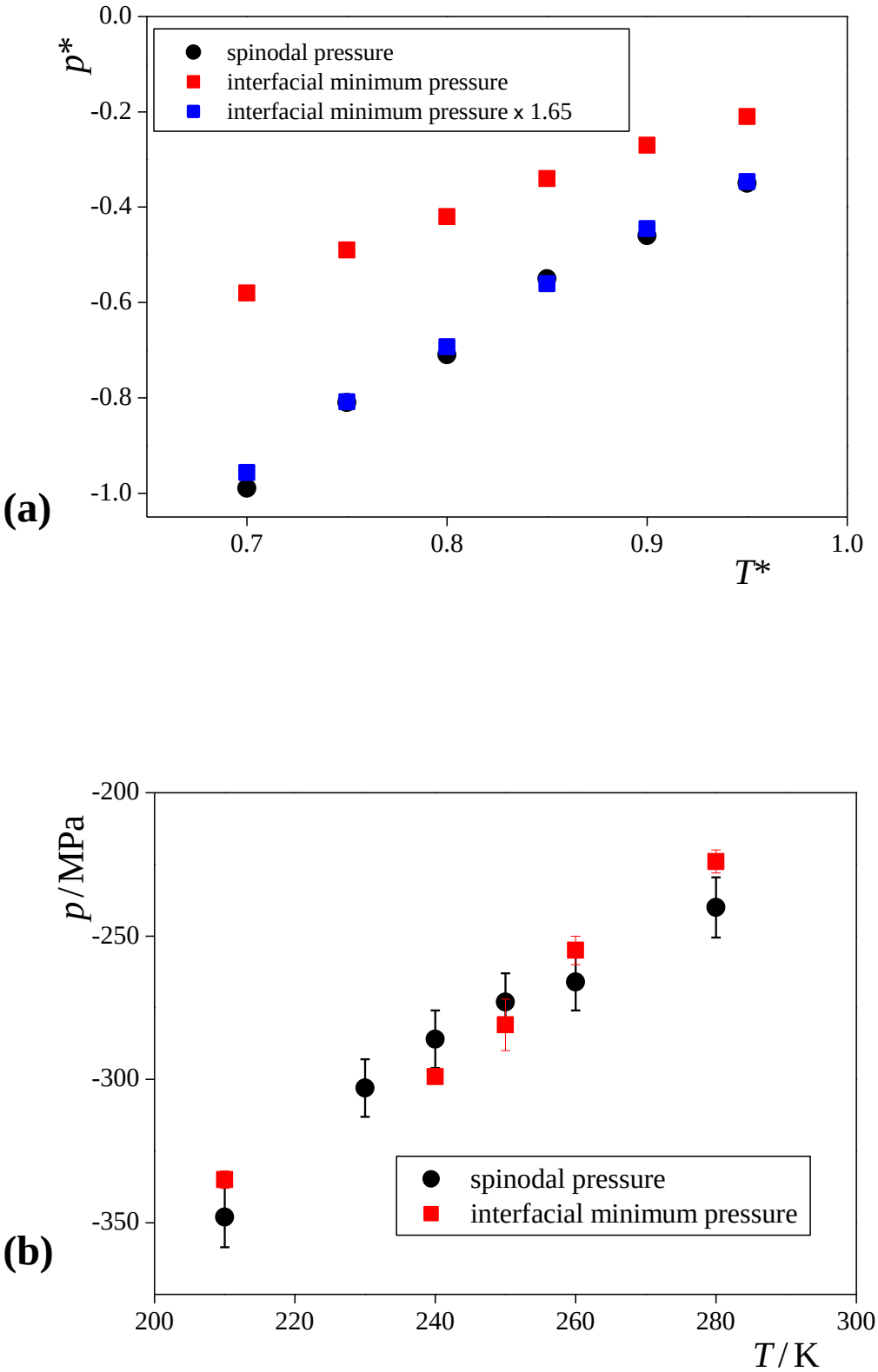

TOC Graphics: